

PAPER • OPEN ACCESS

Design Optimization of Structural Parameters for Inductive Magnetic Sensor

To cite this article: Jie Zhao *et al* 2019 *IOP Conf. Ser.: Mater. Sci. Eng.* **490** 072051

View the [article online](#) for updates and enhancements.



IOP | ebooks™

Bringing you innovative digital publishing with leading voices to create your essential collection of books in STEM research.

Start exploring the collection - download the first chapter of every title for free.

Design Optimization of Structural Parameters for Inductive Magnetic Sensor

Jie Zhao^{1,2}, Zhicheng Wang^{1, 2,*}, MD RAYHAN Tanvir², Shumin Zhou^{1,2}, Hongwei Huang¹

¹School of Mechanical and Electronic Engineering, East China University of Technology, Nanchang Jiangxi 330013, China

²Jiangxi Engineering Research Center for New Energy Technology and Equipment, Nanchang Jiangxi 330013, China

*Corresponding author e-mail: 277732648@qq.com

Abstract. In recent years, the national electric power industry has developed rapidly, the power system is becoming more and more perfect, the modern transmission network is constantly developing and building, the digital substation is gradually intellectualized and the fast fault location of the power system has become the main focus development of the smart grid. A magnetic induction traveling wave sensor is designed for high voltage power fault line traveling wave band frequency bandwidth, easy saturation, fast signal attenuation, poor transient characteristics and serious electromagnetic interference. The magnetic field simulation and signal analysis are carried out based on Ansoft Maxwell and Matlab software platform. The relationship between the structural parameters of the sensor and the electrical characteristics of the sensor is established by combining the theoretical research with the experimental verification. The structural parameters such as the core, the number of coil turns and the line diameter are optimized and the sensitivity of the sensor is improved and the development of the new sensor is completed. The research results show that the optimized sensor can pick up 100 KHz – 10 MHz traveling wave signal accurately and has high transmission ratio, high attenuation and strong interference suppression ability.

1. Introduction

The fast fault location technology can reduce the burden of traditional artificial patrol method of high voltage power line, reduce the loss of fault and shorten the time of repair. It has a great significance for the rapid restoration of power supply and the stability of power system [1], so the rapid fault location has been widely used. There are many kinds of fault location method [2] available for the transmission line. The traveling wave distance measuring method has the advantages of fast traveling wave speed which is close to the speed of light. It is not influenced by system operation mode, system oscillation, line type, transition resistance and line distribution capacitance. It has become one of the hot concepts in the present time of this field.

At present, the traveling wave sensing technology has such problems like easy saturation, poor transient characteristics and serious electromagnetic interference [4] and magnetic induction sensing technology has the characteristics of technical maturity, good high frequency response, high sensitivity, low cost, high efficiency and so on which is very suitable for locating fault of the traveling waves [5].



The transfer capability and sensitivity of the sensor are determined by the coil number, diameter and magnetic core of the magnetic induction sensor. In order to optimize the sensitivity and other properties of the sensor, the theoretical research and simulation analysis of the optimization design method for magnetic induction sensor structure parameters are carried out and also the experimental verifications has been done.

2. The principle of magnetic induction traveling wave sensors

The magnetic induction traveling wave sensor is made by nickel zinc (NiZn) ferrite core which has high resistivity, low loss, high cut-off frequency and high sensitivity, uniformly dense winding coils with proper number of turns and made with special electromagnetic shield and pressure resistance and insulation treatment. Its structure is shown in Figure 1.

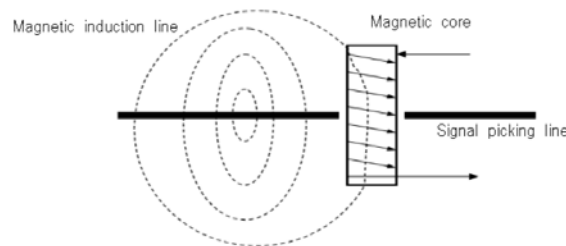


Fig 1. Sensor structure schematic diagram

As shown in Fig. 1, based on Faraday's law of electromagnetic induction, the induced electromotive force [6] generated by a magnetic induction coil is:

$$E = NA_c \frac{dB}{dt} = \frac{NS\mu_e}{2\pi r} \cdot \frac{di(t)}{dt} \quad (1)$$

In equation (1), N is the number of the coil turns, AC is the cross section of the coil, B is the magnetic induction intensity parallel to the core, μ_e is the effective permeability, $i(t)$ is the exciting current and r is the distance between the coil and the feeder.

For sensitivity analysis, the sensitivity Ψ [7] is introduced and its frequency domain expression is:

$$\psi = \left| \frac{E}{B} \right| = j\omega NA_c \quad (2)$$

In this equation, ω the angular frequency and j is the complex number.

In order to improve the sensitivity of the sensor, the induction electrodynamics potential which mainly depends on the magnetic permeability, cross sectional area of the coil and number of turns of the coil should be improved as much as possible when the magnetic induction intensity of the measured magnetic field is fixed. Therefore, how to improve μ_e , A_c and N harmony effectively is the key to sensor performance optimization.

3. Structural parameters optimization design of magnetic induction traveling wave sensor

3.1 Optimum design of effective permeability for core

3.1.1 Theoretical study on effective permeability of magnetic core. According to the theory of electromagnetism, the main function of magnetic core material is to increase the effective permeability of magnetic core [8], and suppress high-frequency noise interference and harmonic interference. NiZn ferrite has been widely used for its high cut-off frequency, high resistivity, low magnetic core loss, good temperature stability, simple sintering process, low cost and so on [9]. The equation (1) shows that in order to improve the electromotive force induction of the sensor, the effective permeability of the core needs to be improved as much as possible, and the effective permeability of the core is related to the size of the core (length to diameter ratio λ) and the initial permeability of the core and the relationship between the long cylinder μ_e , μ_0 and λ is shown in figure 2[10].

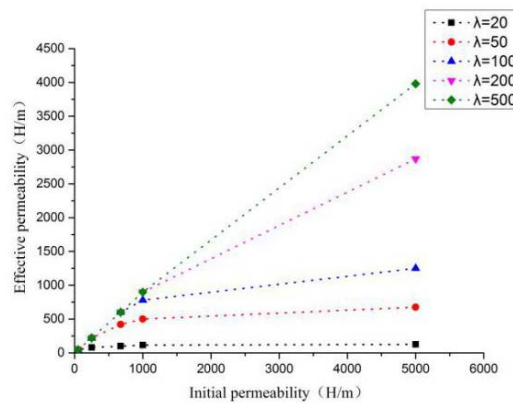


Fig 2. The relationship between μ_e , μ_0 and λ

As it can be seen from figure 2, when the initial magnetic permeability is same, the ratio of length to diameter is larger, the effective permeability is greater and the initial magnetic permeability is also greater. The greater the initial permeability, the greater the effective permeability but the permeability will be saturated when the initial permeability reaches a certain order of magnitude. From the flatness of the curve, the magnetic core size has greater influence on the effective permeability of the core than the initial permeability of the magnetic core.

3.1.2 Experiment verification of initial permeability of magnetic core. In actual design, taking into account the volume of the magnetic core installation slot [11], the rod ferrite NiZn with long 100 mm and diameter 10 mm is chosen as core of the sensor. In the case of some other parameters, the magnetic induction sensors of 40, 60, 100 and 400 are fabricated with initial permeability respectively. Four sensors are tested repeatedly using the traveling wave simulation system which is shown in figure 3 and the waveforms of wave test are shown in figure 4.

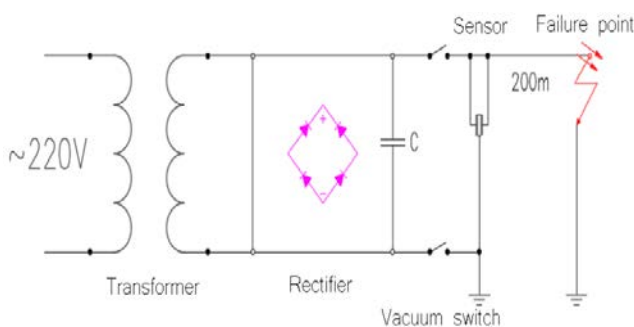


Fig 3. Traveling wave simulation

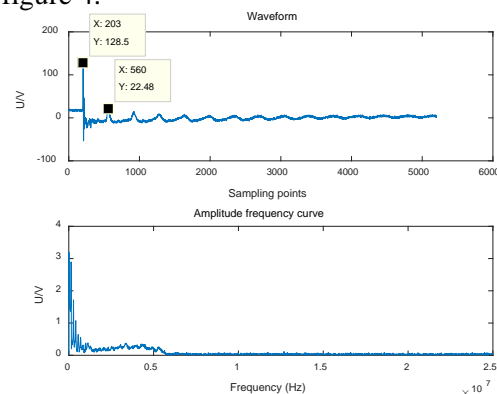
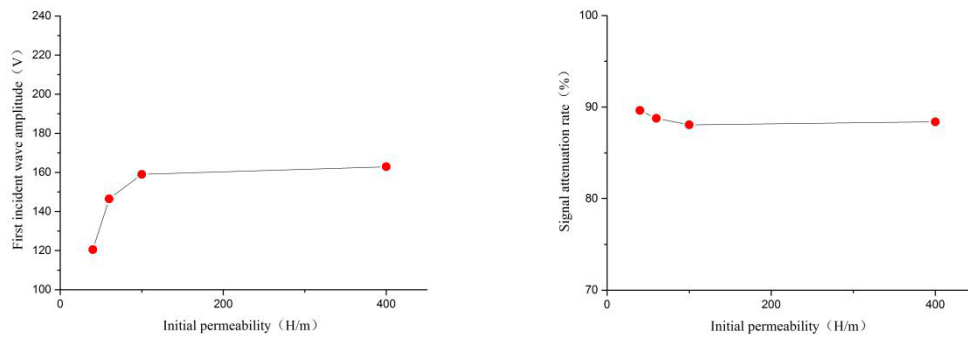


Fig 4. Traveling wave test signal

As it can be seen in figure 4, the magnetic induction traveling wave sensor has a stable high frequency response and the main components of the signal are concentrated in 100 KHz ~ 10 MHz. Based on the Matlab software platform, the waveform data of four kinds of traveling wave sensors with different initial permeability are analyzed and the obtained results are shown in figure 5.



(a) The amplitude of the initial wave

(b) Signal attenuation rate

Fig 5. Influence of initial permeability on signal transmission characteristics

It can be seen from figure 5(a) that the induced electromotive force increases with the increment of the core's initial permeability. When the initial permeability is less than 100, the trend of the electromotive force induction is more obvious but when the initial permeability is over 100, the electromotive force induction remains unchanged and the core is saturated. From figure 5(b), it can be seen that the initial permeability of the core does not affect the attenuation of the signal basically. The signal attenuation below four of the initial magnetic permeability is basically the same and the error is not more than 1%. Therefore, when the NXO-100 with a length to diameter ratio of 10 is selected as the selected as the core, the sensor has a high sensitivity and the same induced electromotive force can be transmitted high under the same exciting current and the attenuation rate of the signal is minimum.

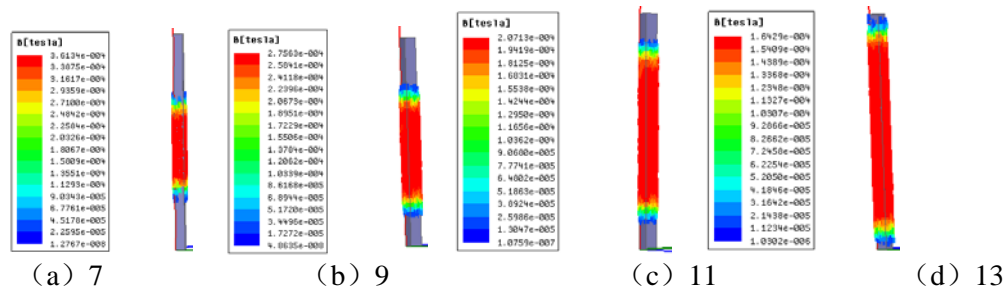
3.2 Optimum design of coil turns

According to the equation (2), in order to obtain greater sensitivity, the number of coil turns need to be increased. If the number of turns is too small, which leads the electromotive force induction is too small and the traveling wave signal cannot be collected [12]. But, According to the equation (3), the magnetic saturation of the core will be induced when the coil reaches a certain turn and the induced electromotive force will not continue to increase. Therefore, the optimization design of coil turns is particularly important.

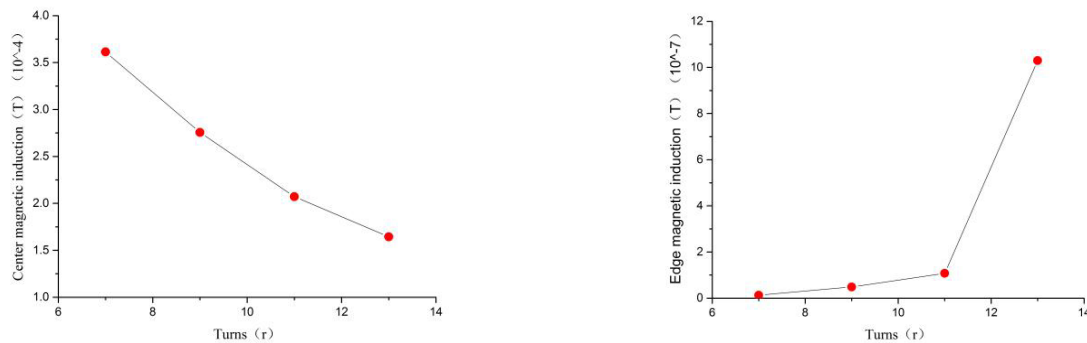
$$\lim_{N \rightarrow \infty} (N\eta) = (N\eta)_{ext} \quad (3)$$

In this equation, N is the number of turns for the coil, η is the coupling coefficient of the coil and core.

3.2.1 Simulation analysis of the number of coil turns. According to the results of the 3.1 section, NXO-100 is selected as the core and the magnetic induction intensity of different number of coil sensors is simulated on the Ansoft Maxwell software platform and the approximate range of the coil number is determined according to the influence factors of the sensors sensitivity. Figure 6 is a simulation diagram of magnetic induction intensity for 7 cores winding with 9 turns, 11 turns and 13 turns.

**Fig 6.** Magnetic induction intensity distribution diagram under different number of turns

From figure 6, it can be seen that the magnetic induction intensity distribution of the magnetic cores with different turns in Ansoft Maxwell simulation is different and the central magnetic induction intensity and the edge magnetic induction intensity are analyzed in detail, as shown in figure 7.



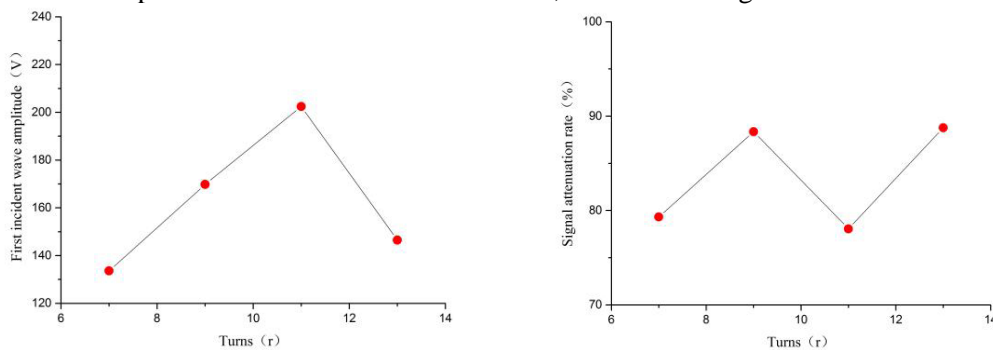
(a) Central magnetic induction intensity

(b) Edge magnetic induction intensity

Fig 7. Magnetic induction intensity curve diagram under different number of turns

From figure 7, it can be seen that the central magnetic induction intensity decreases with the increase of the number of coil turns, that means, the central magnetic induction intensity is inversely proportional to the number of coil turns and the edge magnetic induction intensity increases with the increase of the number of coil turns and there is a sharp increase when the coil number is more than 11 turns. Therefore, when the number of turns is 11, the magnetic core has strong magnetic induction intensity everywhere and the sensor has higher sensitivity and better transmission ability.

3.2.2 Experimental verification for turn numbers of coil. In order to further verification of the correctness of the simulation, the magnetic induction sensors with 7 turns, 9 turns, 11 turns and 13 turns are made respectively with the same parameters and 4 sensors are tested repeatedly using the traveling wave simulation experiment system shown in Figure 3 and the results are analyzed based on the Matlab software platform. The results are as follows, as shown in Figure 8.



(a) The amplitude of the initial wave

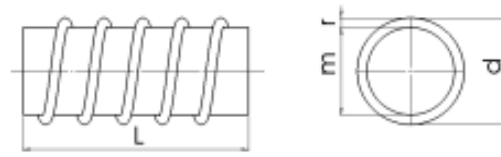
(b) Signal attenuation rate

Fig 8. Different number of signal analysis law curve

As can be seen from figure 8(a), the electromotive force induction and coil winding has nonlinear changes. When the number of coil turns is less than 11, the electromotive force induction increases with the number of coil turns and when the turn numbers of coil is over 11, the induction electromotive force decreases with the number of coil turns and the attenuation degree is larger. It can be seen from 8(b) that when the number of coil turns is 11, it's not only has the minimum attenuation rate but also the wave head of the second incident wave is 22.41V, which is much higher than that of several volts under other turns and it is easy to identify. Therefore, the experimental results are consistent with the simulation results. When the coil is at 11 turns, the sensor is shown the best performance, the highest sensitivity and the strongest transmission capability.

3.3 Optimization design of coil line diameter

The coil structure of the magnetic induction traveling wave sensor is shown in figure 9.



(a) Windings (b) Cross Sectional area

Fig 9. Coil structure diagram

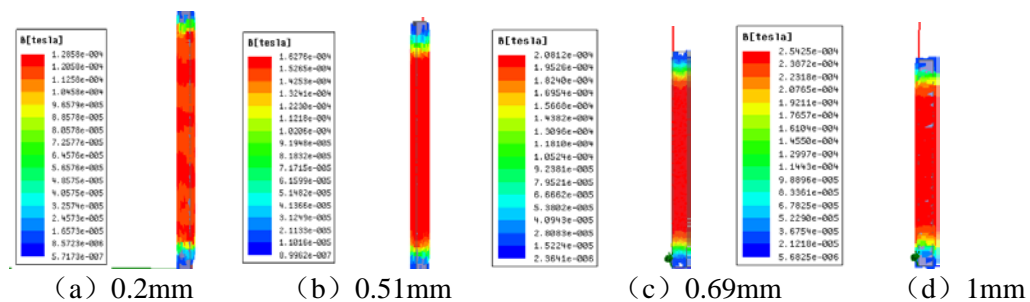
The cross sectional area of the coil A_c can be expressed in equation (4):

$$A_c = \frac{\pi d^2}{4} = \frac{\pi(m + 2r)^2}{4} \quad (4)$$

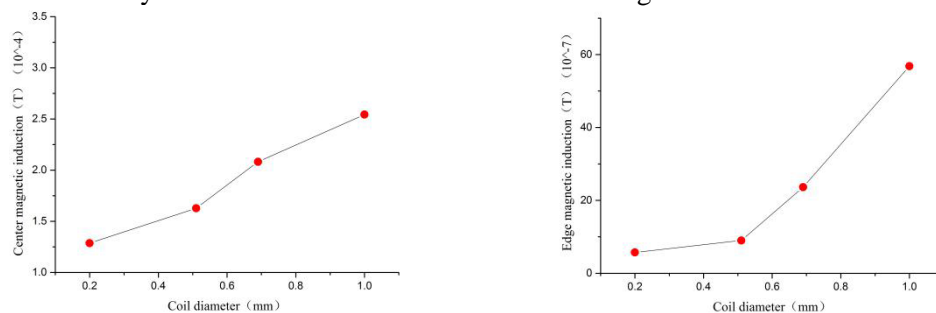
Here, L is the length of the core, m is the diameter of the core, d is the equivalent section diameter of the coil and r is the diameter of the coil.

As shown in the equation (4), the cross sectional area of the coil will also increase with increases of the diameter of the coil. In order to obtain greater sensitivity, the larger the line diameter, the better the result, but the line diameter over the assembly affects the sensors sensitivity, so the study of the optimal line diameter of the receiving coil is particularly important.

3.3.1 Simulation analysis of coil line diameter. According to the analytical results of the 3.2 section, the magnetic induction intensity of the coil with diameter of 0.2 mm, 0.51 mm, 0.69 mm and 1 mm is simulated respectively and the results are shown in figure 10.

**Fig. 10** Magnetic induction intensity distribution diagram under different wire diameter

The central magnetic induction intensity and the edge magnetic induction intensity under different turns are analyzed in details. The results are shown in figure 11.



(a) Central magnetic induction intensity (b) Edge magnetic induction intensity

Fig 11. Magnetic induction intensity curve diagram under different wire diameters

From figure 11, it can be seen that both the central magnetic induction intensity and the edge magnetic induction intensity decrease with the increase of the line diameter that means the magnetic induction intensity of the core is directly proportional to the coil diameter. But both theory and research shows that the threshold sensitivity depends on the area of the coil [13] and the area of the coil is directly proportional to the diameter of the coil. In order to improve the sensibility and enhance the transmission ability of sensors, the magnetic flux density of magnetic cores should be greater than each other. Therefore, the coil of 0.69 mm is the best choice.

3.3.2 Experiment verification. In order to verify the correctness of the simulation, the magnetic induction sensors of 0.2 mm, 0.51 mm, 0.69 mm and 1 mm are made in the same conditions as the magnetic core and the number of turns and all the 4 sensors are tested repeatedly by the traveling wave simulation experiment system shown in figure 3 and the experimental results are split on the Matlab software platform. The results of the analysis are shown in figure 12.

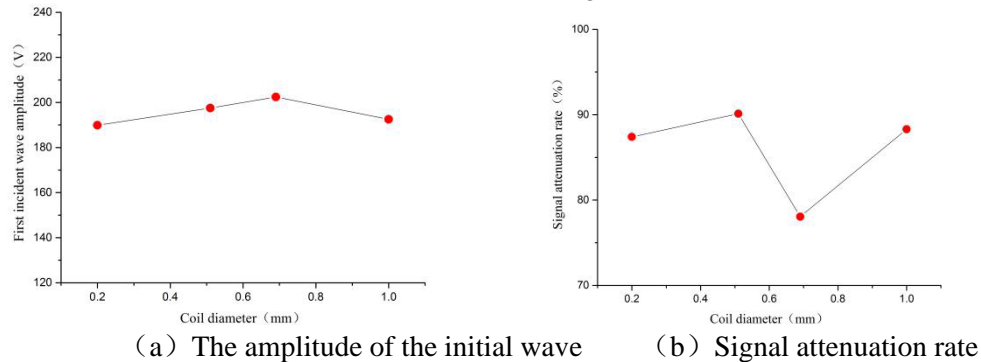


Fig 12. Different line signal analysis law curve

From figure 12(a), it can be seen that when the number of coil optimization turns is determined, after changing the line diameter the performances of the 4 traveling wave sensors are shown better and the increase of electromotive force induction is relatively small, which basically meets the change trend under the theoretical analysis. Also from figure 12(b), it can be seen that the signal attenuation of the sensor made by the other lines is very large except the signal attenuation of the sensor made by 0.69 mm is small and one time reflection of the incident wave attenuates by 90%. Therefore, the experimental results are consistent with the simulation results. The sensor has the best performance when the diameter is 0.69 mm. Comprehensive figure 8 and 12 shows that the change of coil turns has a great influence on the signal transmission ratio, while the change of coil diameter has a greater impact on signal attenuation.

4. Conclusion

Based on Ansoft Maxwell and Matlab software platform, through theoretical research and experimental verification, the curves of various sensor structural parameters on their electrical characteristics are obtained. When the length and diameter ratio of core $\lambda=10$, the initial magnetic core permeability $\mu_0=100$, the coil number $N=11$ and the line diameter is 0.69 mm, the sensor has the best performance, highest sensitivity, strongest transmission capacity and the least attenuation of the signal which achieves the purpose of optimizing the sensor performance.

Acknowledgements

The project is sponsored by the Jiangxi science and technology project (20121BBG70062), the Education Hall technology landing program (KJLD13050), and the open fund (JXNE2016-15) of the Jiangxi new energy technology and equipment Engineering Technology Research Center (JXNE2016-15). The formulation of the experimental scheme and the measurement and record of the experimental data were completed by the staff of Xiao Ruzhi, Jiang Shouqiang and Liao Fang of the Donghua Polytechnic University and expressed the sincere thanks to them.

References

- [1] HE Junna, CHEN Jianyun, AI Yingmei, FENG Qiushi. Traveling wave distance measurement method and development in power system [J]. Power System Protection and Control, 2014, 42(24): 148-154.
- [2] CAOYi. Research on fault location method for complex transmission lines [D]. Nanjing University of Science and Technology, 2014.
- [3] YAO Jinxiong. Research on fault wave recording device for power transmission lines [D]. Xi'an University of Technology, 2014.
- [4] ZHU Huofeng. Travelling wave fault location technology for transmission line based on

- electronic transformer in smart substation [D]. Shan Dong University, 2010.
- [5] YE Jichuan. Research on traveling wave ranging of single phase earth fault in distribution network [D]. Hebei University of Technology, 2012.
- [6] WU Qilin, YU Honglin. The principle of multi-electromagnetic detector based on ring ball grid [J]. Journal of Chongqing University of Technology (Natural Science), 2012, 26(06): 89-94.
- [7] SHAO Yingqiu. Development of Broadband Inductive Magnetic Sensor [D]. Jilin University, 2012.
- [8] JIANG Anlin, ZHOU Suihua, ZHANG Xiaobing, Chen Zhiyi. Inductive magnetic sensor design [J]. Ship Electricity Technology, 2011, 31(12):35-37.
- [9] YAN Bin, SU Hua, ZHANG Huaiwu. The type and application of NiZn soft ferrite material [J]. Core Materials and Devices, 2008(03):48-51.
- [10] CHEN Xingpeng. Research on AMT magnetic field sensor [D]. Central South University, 2012.
- [11] SHAO Yingqiu, CHENG Defu, WANG Yanzhang, ZHANG Fei. Research on high sensitive inductive magnetic sensors [J]. Journal of Instrument and Instrument, 2012, 33(02):349-355.
- [12] CHEN Xingpeng, SONG Gang, ZHOU Sheng, XI Zhenzhu. Development of audio Magnetotelluric Magnetic Field Sensor [J]. Chinese Journal of Nonferrous Metals, 2012, 22(03):922-927.
- [13] LIU Jiabin, YANG Lijian, CHEN Peng. Selection of eddy current displacement sensor probe parameters [J]. Success (education), 2007(09):223.